

Crystallization and crystal structure of lysozyme in the presence of nanosized Titanium dioxide

H. I. Sbirikova-Dimitrova^{1*}, S. Georgieva², V. Ganev¹, B. L. Shivachev¹

¹ Institute of Mineralogy and Crystallography “Acad. Ivan Kostov”, Bulgarian Academy of Sciences, Acad. G. Bonchev str., bl. 107, 1113 Sofia, Bulgaria

² University of chemical technology and metallurgy, 8 Blvd. Kl. Ohridski, Sofia 1756, Bulgaria

Received October 31, 2018; Accepted November 19, 2018

We present a single crystal XRD, LA-ICP-MS and cyclic voltammetry studies on the observed interaction of the protein lysozyme and TiO₂ nanosized particles (JRC NM-101, anatase). The diffraction quality of lysozyme single crystals grown in presence and absence of TiO₂ was comparable. The X-ray structure solution revealed that lysozyme crystallizes in the *P*4₃2₁2 space group and disclosed the presence of electron density that was assigned to Na⁺ and Ti⁴⁺ ions. LA-ICP-MS analyses were conducted on both lysozyme-TiO₂ single crystals and SDS-PAGE featuring lysozyme-TiO₂ interaction. LA-ICP-MS data confirmed the presence of Ti⁴⁺ ions and the increased concentration of Na⁺. Cyclic voltammetry and differential pulsed polarography results suggest that titanium binds successfully with the enzyme and that the complex formation is irreversible, at least in slightly acidic conditions (pH 6.5).

Keywords: lysozyme, TiO₂ nanoparticles, single crystal, XRD, LA-ICP-MS.

INTRODUCTION

Engineered nanomaterials (ENM) are entering more and more in our surroundings while the existence or absence of effects on the environment (ecotoxicity etc.), on human health (uptake, release, interaction, nanotoxicity, nanogenotoxicity etc.) remains questionable [1–4]. Though TiO₂ is supposedly to be “inert”, several studies have detected the presence of Ti⁴⁺ ions in human blood mainly in patients with titanium implants [5, 6]. The detection of “ionic” titanium is largely related to the corrosion of implants in such patients and yet its presence cannot be clearly explained or understood as the concentration are higher than anticipated [7, 8]. Nanosized titanium dioxide is used in sun creams as UV filter [9], as supplement for whitening and brightening foods [10], as catalyst for degradation and treatment of wastewaters and pesticides [11] etc.

Nowadays crystallization of Hen egg white (HEW) lysozyme is easily achievable as it is routinely used as a model system [12, 13]. Usually the crystallization of a protein is a function of several parameters starting from the “solution” (purity, pH, additive(s), concentrations of protein and/or salts,

etc.) and even small changes or variations can undermine successful outcomes [14–16]. In this paper we report data for crystallization of HEW lysozyme in the presence of TiO₂ nanoparticles, crystal structure solution and observed presence of Ti⁴⁺ ions in the HEW lysozyme single crystals and mixtures. The crystallization experiments were performed using constant lysozyme concentration and buffer, the only variation was the presence or absence of TiO₂ nanoparticles. The observation of structural and chemical adjustments was assessed by single crystal diffraction, LA-ICP-MS and cyclic voltammetry.

EXPERIMENTAL

Sample crystallization

The enzyme HEW lysozyme was crystallized by the hanging drop vapor diffusion method. The initial crystallization conditions included 20 mg/ml lysozyme (Sigma L6876) in absence or presence of TiO₂ 2.56 mg/ml (JRC NM-101, [17]), well/solution: 10% w/v sodium chloride (NaCl), 0.1M sodium acetate (C₂H₃NaO₂) buffer (pH 5.0), 25% (v/v) ethylene glycol (C₂H₆O₂). The drop size was 4 μl (2 μl Lys + 2 μl well solution). Crystallization plates were stored in controlled temperature rooms (16–20°C). Large crystals (0.4 x 0.35 x 0.35 mm³)

* To whom all correspondence should be sent:
E-mail: sbirikova@mail.bg

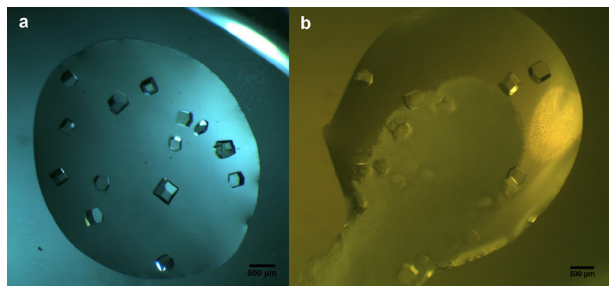


Fig. 1. Obtained Lysozyme single crystals *a*) in absence of TiO_2 and *b*) in presence of TiO_2 (TiO_2 is the white dispersion).

suitable for single crystal X-ray analysis, formed within a month (Fig. 1).

Data collection and crystal structure refinement

The obtained crystals were colorless (Fig. 1) and diffracted up to 1.8 Å resolution. Crystals were mounted on loops and were flash frozen at 130 K directly under the nitrogen cryo stream (Cobra, Oxfordcryosystems). All data were collected at low temperature (130 K) on an Oxford diffraction Supernova diffractometer using Cu-K α radiation ($\lambda = 1.54056$ Å) from micro-focus source. The determination of unit cell parameters, data integration, scaling and absorption correction were carried out using the CrysAlisPro software [18]. The phases were obtained by molecular replacement with Phaser [19] using 1DPX [20] as starting model. The refinement of the structure involved several cycles of refinement using Refmac [21] and Coot [22] programs. The water and heavier atoms (Ti, Cl and Na) were positioned on the *Fo-Fc* difference map using the interface of Coot program [22]. A summary of the fundamental crystal data and refinement indicators is provided in Table 1. Graphical analyses of the model, the electron-density maps and the figures were carried out using programs Coot [22] and PyMOL [23]. The coordinates and structure factors have been deposited in the PDB as entry **6G5C**.

Cyclic Voltammetry (CV) and Differential Puls Polarography (DPP)

The voltammograms (CV and DPP) were recorded on a Metrohm 797 VA trace analyzer and a 797 VA stand. The Ag/AgCl, (3 mol l⁻¹) KCl electrode was used as the reference electrode, the static mercury drop electrode as the working electrode, and the carbon electrode as the auxiliary electrode. A 0.1 mol l⁻¹ sodium tartrate buffer solution (pH 6.5 ± 0.1) was used as a supporting electrolyte. The stock solutions of TiO_2 (0.002088 mol l⁻¹) and

Table 1. Selected crystallographic data-collection statistics and refinement indicators for **6G5C**

Crystal system	Tetragonal
Space group	$P4_32_12$
<i>cell dimensions</i>	
<i>a, b, c, Å</i>	78.87, 78.87, 36.89
$\alpha, \beta, \gamma, ^\circ$	90, 90, 90
independent molecules	1
<i>diffraction data</i>	
wavelength, Å	1.54056
resolution, Å	1.8
reflections	11235
completeness, %	99.7
<i>I/σ(I)</i>	11.68
Redundancy	8.2
<i>Rmerge</i> %	16.6(20.4)
<i>Refinement</i>	
reflections used	10691
resolution, Å	1.8
<i>no. of atoms</i>	1120
Amino Acids (protein)	1000
Ti, Na, Cl/ion, EDO	16
waters	104
average B factor, Å ²	10.0
<i>R.m.s.d.</i>	
bond lengths, Å	0.019
bond angles, °	1.855
PDB code	6G5C

lysozyme (ligand) (0.01303 mol l⁻¹) were prepared by dissolution of TiO_2 in 7% H_2SO_4 and lysozyme in distilled and sterilized water. A working solution was prepared mixing TiO_2 and lysozyme in concentrations 0.001044 mol l⁻¹ and 0.002088 mol l⁻¹ ($n\text{Ti (mmol)} : n\text{Lys (mmol)} = 1 : 2$) in sodium tartrate buffer (0.1 mol l⁻¹; pH 6.5). All used reagents were of analytical grade.

Procedure

Cyclic voltammetry. A 6 ml volume of tartrate buffer and 20 µl of TiO_2 stock solution were pipetted in the electrochemical cell. Oxygen was removed by bubbling of pure nitrogen through the solution for 10 minutes. The voltammogram was registered at the follow parameters: working electrode: HMDE, Voltage step 5 mV, Sweep rate 0.500 mV s⁻¹. 10 µl of the stock solution containing lysozyme was introduced in the cell. The solution was purged with nitrogen for 5 min and the analytical signal was registered.

Differential Puls Polarography: A 20 µl of the titanium stock solution and 6 ml tartrate buffer were

mixed and after that oxygen was removed by passing nitrogen gas for 10 min. The cathodic peak of Ti(IV) was registered at a static mercury dropping electrode (SMDE), amplitude -50 mV, voltage step 5 mV, voltage step time 0.4 s and scan rate of potential -12.6 mV s $^{-1}$. Volumes from 10 to 40 μ l of the working solution of the complex Ti(IV)-Lys and volumes of 10 to 300 μ l of the stock ligand solution were introduced in the electrochemical cell. After each Ti(IV)-Lys volume was added the solution was purged with nitrogen for 10 min. The analytical signal was registered and the peak potential and the current were measured.

Laser Ablation Inductively Coupled Plasma Mass Spectrometry (LA-ICP-MS)

The qualitative content of Ti $^{4+}$ and Na $^{+}$ was determined by laser ablation inductively coupled plasma (LA-ICP-MS) measurements. The measurements were performed on PerkinElmer ELAN DRC-e ICP-MS instrument in standard mode integrated with New Wave Research (ESI) UP-193FX ArF excimer laser ablation system in single ablation spot setup (laser energy 7.5 mJ; repetition rate 10 Hz; spot size 50 μ m). Optimized dry plasma conditions are obtained by precisely controlled carrier (He) and make-up (Ar) gas flows. MFC is used for ablation chamber environment and carrier gas supply.

Procedure

Single crystals of lysozyme in presence of TiO $_2$ were harvested from the drop and transferred into a drop with crystals not containing TiO $_2$ for 10 – 20 second. This procedure was performed just prior to the LA-ICP-MS experiment. If possible the crystals were washed several time before the LA-ICP-MS

collection. One should note that if excessive “transfer” from drop to drop occurs the single crystals started to degrade. The crystals were fished out of the drop and placed onto a cover slip (18×18 mm) which was immediately introduced into the LA-ICP-MS chamber. The experiment was conducted immediately and a clear spot from the laser ablation was observed (Fig. 2).

The experiments using SDS-PAGE required, after staining and destaining of the gel (Coomassie blue), to cut pieces of the gel (with protein). Two types of positioning of the cut samples were performed: one was flat and the other one included a 90° tilt so that the laser could be focused in the “thin” part of the gel (Fig. 2a). Then the cut pieces were introduced into the LA-ICP-MS chamber and the experiment was conducted.

RESULTS AND DISCUSSION

Currently, studies involving the interaction of nanomaterials with biological molecules are becoming more and more routine though the employed protocols and procedures have not been really standardized. Even the preparative procedures of ENM for routine analyzes using commonly employed methods for physico-chemical characterization (TEM, ICP, SEM, DLS etc.) vary between laboratories and are prone to empirical adjustment. It is interestingly to note that dispersion protocol of ENM may include the presence of protein, supposedly acting as surfactant or coating [17, 24]. Though different methods can be employed for detecting quantitatively and qualitatively protein-ligand interaction, only NMR and diffraction techniques can provide structural insights. On the other hand it is difficult to draw information regarding the chemical composition based solely on NMR or diffraction techniques. Thus a combination of methods and techniques must be envisaged to ascertain the interaction from both structural and chemical approach. Nowadays the procedure of lysozyme crystallization has been nearly perfected and thus it is well suited for crystallographic studies. We have exploited this robust crystallization “know-how” as model system in order to assess the interaction between TiO $_2$ and lysozyme. The concept was just to ascertain or reject a possible interaction between nanosized TiO $_2$ and lysozyme (as a model). Several similar studies on protein-nanosized materials have been conducted, aiming at detecting the crystallization role of protein [25–27] or the absorption of the protein on the surface of the nanomaterial [28, 29]. The employed in this study nanosized anatase (e.g. JRC NM-101) has also been thoroughly characterized Fig. 3 and ref. 17.

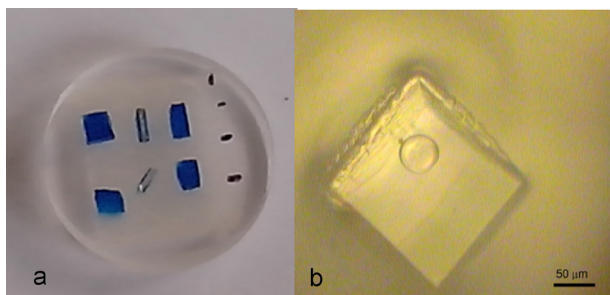


Fig. 2. LA-ICP-MS samples *a*) cut pieces of the gel with different orientations: surface of the gel and tilted by 90° exposing the inside of the gel and *b*) Lysozyme single crystal after laser ablation; the spot of the ablation is well preserved and no crystal degradation is observed.

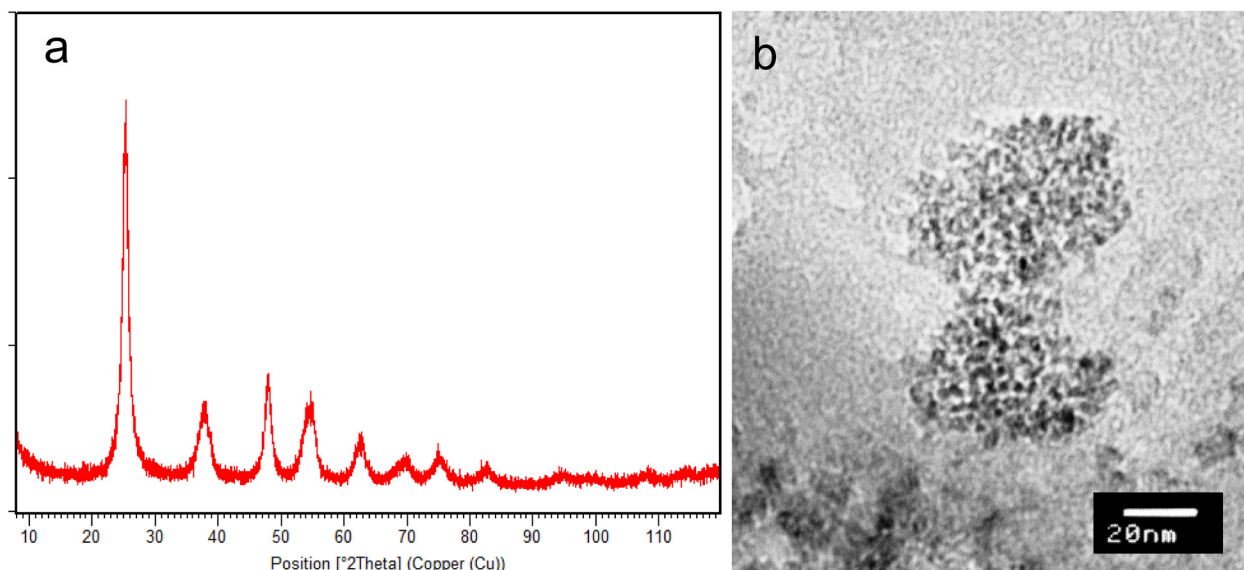


Fig. 3. Collected *a*) powder diffraction pattern of employed anatase NM-101 and *b*) TEM micrograph showing that the particle size is below 20 nm (reproduced from ref. 17).

Single crystal data collection has been attempted for several different crystals. One should note that the dataset collected diffracted to a resolution of 1.8 Å and was from a crystal that was harvested from the drop ten (10) days after it was spotted. Crystals with similar or even bigger dimensions (size) that were allowed to “stabilize” for more than a month in the crystallization drop diffracted usually at resolution up to 2.5 Å. Attempts for data collection at room temperature (19 °C) were performed on a few crystals, however observed quality of the diffraction was not comparable with that for experiments conducted at 130 K. The presence of Titanium dioxide in the crystallization conditions may have played a role for the rapid crystal structure stabilization and subsequent destabilization. However, based on the quality of the collected diffraction data, it seems that the introduction of TiO₂ (2.56 mg/ml) to the crystallization conditions has no or very little effect on the lysozyme crystal growth. The structure solution showed that 6G5C corresponds to a classical C-type lysozyme [12, 20]. The asymmetric unit of 6G5C consists of one lysozyme molecule and comprises 104 water solvent molecules. Some of these waters are first hydration-shell, ordered and well defined. In addition the *F_o-F_c* difference map, suggests the presence of heavier atoms (heavier than water) e.g. Ti⁴⁺, Na⁺ and Cl⁻ ions (Fig. 4). Such inorganic ions as Ti⁴⁺ could, in principle, inhibit the ability of lysozyme to attach to a bacterial cell wall and catalyze lysis [30, 31].

The conducted LA-ICP-MS analyses on the lysozyme+TiO₂ gel and single crystals confirmed the suggested by the XRD presence of Na⁺ and Ti⁴⁺

ions. The LA-ICP-MS analyses showed also that the Na⁺ and Ti⁴⁺ ions were present not only at the surface of the crystals (e.g. as contamination) but also in the bulk. One can clearly see from the analyses that the concentration of both Na⁺ and Ti⁴⁺ ions remains stable even when the ablation resulted from the inside of the single crystal (Fig. 5). The SDS-PAGE analyses included the presence of Na ions (from the Na-dodecyl sulfate) and thus the amount of Na could be adjusted in order to act as internal standard and to allow the quantification of Ti⁴⁺ ions.

The comparison of the LA-ICP-MS data obtained from different single crystals, for the presence or absence of Ti⁴⁺ showed increased amounts of Ti⁴⁺ (Table 2). Interestingly, results for Ti48 and

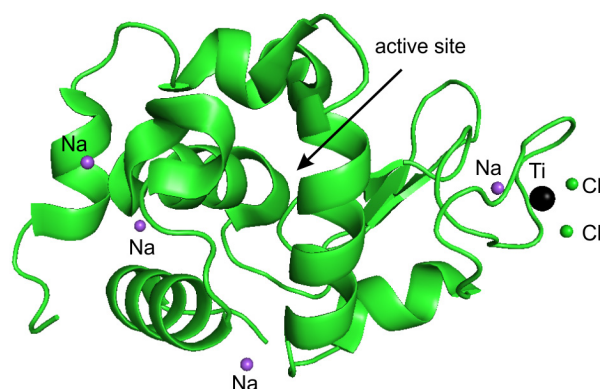


Fig. 4. View of the asymmetric unit of 6G5C (backbone is shown in green color, Ti⁴⁺ in black, Cl⁻ in green, Na⁺ in blue).

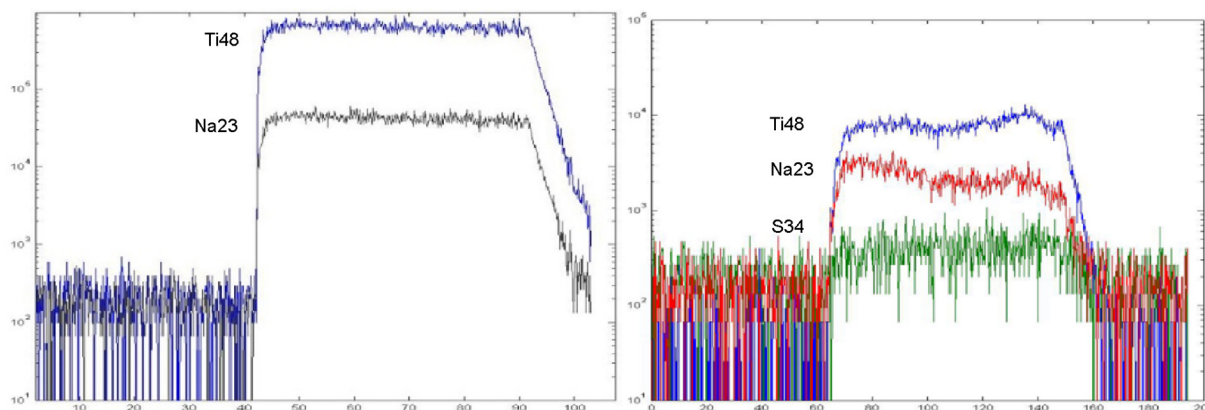


Fig. 5. Representation of LA-ICP-MS data obtained from single crystal (left) and SDS PAGE gel (right) of lysozyme samples in presence of TiO₂.

Table 2. LA-ICP-MS qualitative data for the presence of Ti⁴⁺ obtained from single crystals

Lys+TiO ₂	Single crystal 1	Na23	Ti48	Ti49
spot	sample	µg/g	µg/g	µg/g
3	Proba-2-1	1118.81	26.37	70.62
4	Proba-2-1	1022.12	23.22	40.71
5	Proba-2-1	1582.13	44.68	<LOD
6	Proba-2-1	1333.56	45.37	<LOD
7	Proba-2-1	1443.58	55.10	<LOD
	Average:	1300.04	38.95	55.67
Lys+TiO ₂	Single crystal 2	Na23	Ti48	Ti49
11	Proba-2-90	2369.05	68.16	<LOD
12	Proba-2-90	2283.29	58.21	<LOD
13	Proba-2-90	1948.51	27.48	<LOD
	Average:	2200.29	51.28	n/a
Lys no TiO ₂	Single crystal 3	Na23	Ti48	Ti49
3	Proba-2-1	8.57	1.49	16.19
4	Proba-2-1	6.01	0.93	10.36
5	Proba-2-1	7.35	1.16	<LOD
6	Proba-2-1	8.90	1.54	<LOD
7	Proba-2-1	10.25	2.11	<LOD
	Average:	8.22	1.45	13.28

Ti49 isotopes were not comparable. While based on Ti48 one could detect a 40 fold increase of Ti⁴⁺ the Ti49 data was drifting from a 50 fold increase to lower values e.g. below limit of detection (LOD) for Ti⁴⁺. The observed variations between single crystals may be due to the different time of nucleation and crystal growth, the washing conditions and a plausible degradation of the crystal. Although quantitative, the data also revealed increased amounts of Na⁺ which is also supported by the crystal structure refinement. Indeed in 6G5C there are far more Na

sites compared to similar structures present in the database. The data and its analyses lead to the assumption that one should consider carefully which “Ti” isotope should be used for correct assessment of the interactions.

The LA-ICP-MS on samples cut from the SDS-PAGE gels also suggested a steady interaction between TiO₂ nanoparticles and lysozyme (Table 3). As the PAGE features Na its amounts can be adjusted to allow its use as an internal standard and thus obtain quantitative results. Unfortunately such

Table 3. Quantitative LA-ICP-MS data obtained from SDS-PAGE using Na⁺ as internal standard

Standard	Na23 μg/g	S34 μg/g	Ti46 μg/g	Ti47 μg/g	Ti48 μg/g	Ti49 μg/g
Nist-612-s01	100000.00	<LOD	75.08	39.97	216.06	37.14
Nist-612-s02	100000.00	<LOD	77.80	41.20	213.75	39.86
Lys + TiO ₂	Na23 μg/g	S34 μg/g	Ti46 μg/g	Ti47 μg/g	Ti48 μg/g	Ti49 μg/g
SDS -01	1000.00	<LOD	454.48	489.41	299.17	504.54
SDS -02	1000.00	<LOD	482.94	504.18	306.41	509.78
SDS -03	1000.00	<LOD	561.08	583.90	363.58	607.64
Lys no TiO ₂	Na23 μg/g	S34 μg/g	Ti46 μg/g	Ti47 μg/g	Ti48 μg/g	Ti49 μg/g
SDS-01	1000.00	164544.77	<LOD	<LOD	<LOD	<LOD
SDS-02	1000.00	174465.22	<LOD	<LOD	<LOD	<LOD
SDS-03	1000.00	152881.82	<LOD	<LOD	<LOD	<LOD
BSA no TiO ₂	Na23 μg/g	S34 μg/g	Ti46 μg/g	Ti47 μg/g	Ti48 μg/g	Ti49 μg/g
BSA-01	1000.00	77651.04	<LOD	<LOD	<LOD	<LOD
BSA-03	1000.00	74009.70	<LOD	<LOD	<LOD	<LOD

an experiment has a drawback as it will hide the increase or decrease of lysozyme-Na interaction. While the “absence” of Ti⁴⁺ in the samples without TiO₂ is not surprising the variation of the sulfur amounts is interesting. It is quite clear that when TiO₂ is present in the “condition” the amounts of sulfur (S34) are below the LOD. Such an “interaction” “sulfate-TiO₂” has been already noticed [32, 33]. On the other hand, when no TiO₂ is available the S34 levels are well above the LOD. This may be due to the employed nanosized TiO₂ while if a bulkier material is used the effect may remain hidden.

Cyclic voltamperometry and DPP were used in the study of interfacial and redox behavior of the complex Ti(IV)-Lys and the free ligand (lysozyme) in sodium tartrate buffer (pH 6.5). Cyclic voltammograms for 6.959×10^{-6} mol l⁻¹ Ti(IV) in the presence and the absence of lysozyme (ligand, 1.392×10^{-5} mol l⁻¹) are shown on Fig. 6. The CV of Ti(IV) in sodium tartrate buffer corresponds to the those reported in the literature [34]. Two peaks at $E_{\text{red}} = -1.25$ V and $E_{\text{ox}} = -1.38$ V were observed. After the addition of the ligand (Lysozyme) the cathodic peak was shifted to a more negative potential ($E_{\text{red}} = -1.47$ V) which proves the formation of a complex between Ti(IV) and lysozyme [35]. The immediate reverse potential scan in a positive direction in the presence of Lysozyme in the solution did not produce any anodic peak between -0.70 and -1.7 V indicating that the reoxydation of the

complex between Ti⁴⁺ and lysozyme is irreversible (Fig. 6).

Differential pulps polarography was performed on the ligand solution in the 0.1 mol l⁻¹ tartrate buffer solution (Fig. 7). The profile was similar to the blank voltammogram obtained for the supporting electrolyte solution (0.1 mol l⁻¹ tartrate buffer) with no peaks observed (data not shown) in the scan range of -0.7 to -1.7 V (Fig. 7). Complexation equilibria of Ti-lysozyme system at different concentrations of titanium and lysozyme were also studied by DPP and the voltammograms obtained are shown on Fig. 7. It was found that 10 and 100 fold ligand

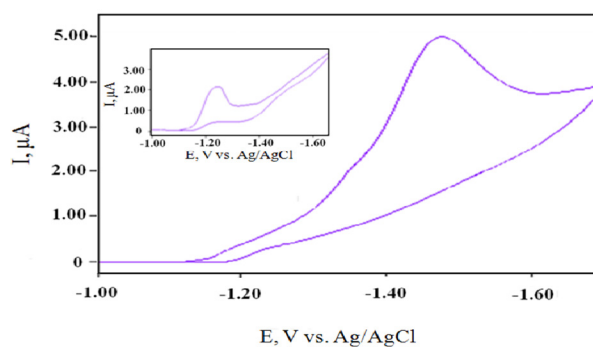


Fig. 6. Cyclic voltammograms of 6.959×10^{-6} mol l⁻¹ Ti(IV) in 0.1 mol l⁻¹ sodium tartrate buffer (inserted graphic) and in presence of 1.392×10^{-5} mol l⁻¹ Lysozyme, scan rate 500 mVs⁻¹.

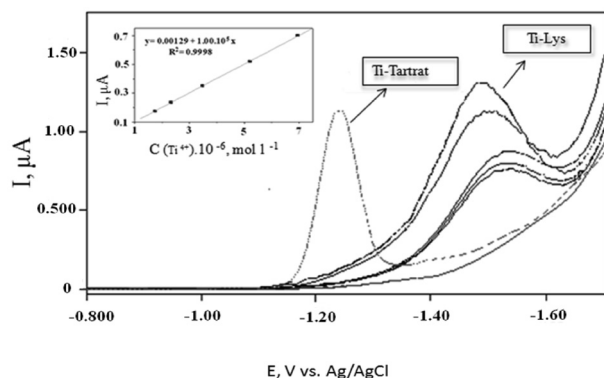


Fig. 7. Differential pulse polarograms: 1) 0.1 mol l⁻¹ sodium tartrate buffer (pH 6.5) (red one curve); 2) Ti(IV) in a solution of 0.1 mol l⁻¹ sodium tartrate buffer (pH 6.5) (blue dotted curve); 3) after ligand (Lysozim) dosing (black curves). Inset picture: graphic and regression equation of the relation $I = f(C_{Ti(IV)})$ after Lysozyme added.

(lysozyme) excess do not exert any effect on the peak height. As expected the peak height of the Ti(IV)-Lys complex increases with the increase of the titanium concentration. Based on the DPP data a correlation between current value and Ti (IV) concentration was established (Fig. 7, inset graph) and the regression equation of $I = f(C_{Ti(IV)})$ was found which proves the diffusion controlled electrode process.

CONCLUSIONS

Single crystals of lysozyme were grown in the presence of nanosized TiO₂. The crystal structure solution at 1.8 Å resolution revealed that Ti⁴⁺ is bound to lysozyme (**6G5C**) and that in addition the Na amounts are increased. The inorganic TiO₂ nanoparticles do not interfere with the Lysozyme biomolecules and do not denatured lysozyme. The LA-ICP-MS data support the increased Na content and the presence of Ti⁴⁺ for both single crystals and even under the more harsh conditions of SDS-PAGE electrophoresis. Differential pulls polarography and CV suggest that the observed interaction between lysozyme and TiO₂ nanoparticles is irreversible, at least for the employed conditions. These results provide an economical and easy route for the synthesis of a wide range of functional bionanocomposites involving nanosized titaniumdioxide.

Acknowledgments: The authors wish to thank Bulgarian Fund for Research Investigations (FNI) for financial support, grant T02/14 and DRNF02/1.

REFERENCES

1. L. Aïnouche, L. Hamadou, A. Kadri, N. Benbrahim, D. Bradai, *Electrochim. Acta*, **133**, 597 (2014).
2. B. R. Levine, A. R. Hsu, A. K. Skipor, N. J. Hallab, W. G. Paprosky, J. O. Galante, J. J. Jacobs, *J. Bone Joint Surg. Am.*, **95**, 512 (2013).
3. B. Smolkova, M. Dusinska, A. Gabelova, *Food Chem. Toxicol.*, **109**, 780 (2017).
4. S. Siegrist, E. Cörek, P. Detampel, J. Sandström, P. Wick, J. Huwyler, *Nanotoxicol.*, **1** (2018).
5. J. P. Curtin, M. Wang, T. Cheng, L. Jin, H. Sun, *J. Biol. Inorg. Chem.*, **23**, 471 (2018).
6. J. J. Jacobs, A. K. Skipor, L. M. Patterson, N. J. Hallab, W. G. Paprosky, J. Black, J. O. Galante, *J. Biol. Inorg. Chem.*, **80**, 1447 (1998).
7. Y. Nuevo-Ordóñez, M. Montes-Bayón, E. Blanco-González, J. Paz-Aparicio, J. D. Raimundez, J. M. Tejerina, M. A. Peña, A. Sanz-Medel, *Anal. Bioanal. Chem.*, **401**, 2747 (2011).
8. M. R. Zierden A. M. Valentine, *Metallomics*, **8**, 9 (2016).
9. K. M. Tyner, A. M. Wokovich, D. E. Godar, W. H. Doub, N. Sadrieh, *Int. J. Cosmet. Sci.*, **33**, 234 (2011).
10. X. Sang, B. Li, Y. Ze, J. Hong, X. Ze, S. Gui, Q. Sun, H. Liu, X. Zhao, L. Sheng, D. Liu, X. Yu, L. Wang, F. Hong, *J. Agricult. Food Chem.*, **61**, 5590 (2013).
11. G. Goutailler, C. Guillard, R. Faure, O. Païssé, *J. Agricult. Food Chem.*, **50**, 5115 (2002).
12. W. Iwai, D. Yagi, T. Ishikawa, Y. Ohnishi, I. Tanaka, N. Niimura, *J. Synchrotron Rad.*, **15**, 312 (2008).
13. C. J. Gerard, G. Ferry, L. M. Vuillard, J. A. Boutin, N. Ferte, R. Grossier, N. Candoni, S. Veessler, *Crystal Growth Des.*, **18**, 5130 (2018).
14. E. Bhat, M. Abdalla, I. Rather, *Glob. J. Biotechnol. Biomater. Sci.*, **4**, 001 (2018).
15. T. M. Bergfors, *Protein crystallization* (International University Line, La Jolla, Calif., 2009), IUL biotechnology series.
16. C. Singh, S. Friedrichs, M. Levin, R. Birkedal, K. Jensen, G. Pojana, W. Wohlleben, S. Schulte, K. Wiench, T. Turney, D. Koulaeva, D. Marshall, K. Hund-Rinke, W. Koerdel, E. Van Doren, P.-J. De Temmerman; F. Abi Daoud, J. Mast, P. Gibson, R. Koeber, Th. Linsinger and Ch. Klein, NM-Series of Representative Manufactured Nanomaterials – Zinc Oxide NM-110, NM-111, NM-112, NM-113: Characterisation and Test Item Preparation, Publications Office of the European Union, 2011.
17. K. Rasmussen, J. Mast, P.-J. De Temmerman, E. Verleysen, N. Waegeneers, F. Van Steen, J.-C. Pizzolon, L. De Temmerman, E. Van Doren, K. A. Jensen Keld, R. Birkedal, M. Levin, S. H. Nielsen, I. K. Koponen, P. A. Clausen, V. Kofoed-Sørensen, Y. Kembouche, N. Thieriet, O. Spalla, C. Giuot, D. Rousset, O. Witschger, Seb. Bau, B. Bianchi, Ch. Motzkus, B. Shivachev, L. Dimowa, R. Nikolova, D. Nihtianova, M. Tarassov, O. Petrov, S. Bakardjieva, D. Gilliland, F. Pianella, G. Ceccone, V. Spampinato, G. Cotogno, P. Gibson, C. Gaillard, A. Mech, Titanium Dioxide, NM-100, NM-101, NM-102,

- NM-103, NM-104, NM-105: Characterisation and Physico-Chemical Properties, Publications Office of the European Union, 2014.
18. A. Technologies, Agilent Technologies UK Ltd Oxford, UK, 2012.
 19. A. J. McCoy, R. W. Grosse-Kunstleve, P. D. Adams, M. D. Winn, L. C. Storoni, R. J. Read, *J. App. Cryst.*, **40**, 658 (2007).
 20. M. S. Weiss, G. J. Palm, R. Hilgenfeld, *Acta Crystallogr. D*, **56**, 952 (2000).
 21. M. D. Winn, G. N. Murshudov, M. Z. Papiz, *Methods in enzymology*, vol. 374, Elsevier, 2003, p. 300.
 22. P. Emsley, K. Cowtan, *Acta Cryst Crystallogr. D*, **60**, 2126 (2004).
 23. The PyMOL Molecular Graphics System, Version 1.6pre, Schrödinger, LLC.
 24. K. Rasmussen, J. Mast, P.-J. De Temmerman, E. Verleysen, N. Waegeneers, F. Van Steen, J.-C. Pizzolon, L. De Temmerman, E. Van Doren, K. A. Jensen, R. Birkedal, P. A. Clausen, Y. Kembouche, N. Thieriet, O. Spalla, C. Giuot, D. Rousset, O. Witschger, S. Bau, B. Bianchi, B. Shivachev, L. Dimowa, R. Nikolova, D. Nihtianova, M. Tarassov, O. Petrov, S. Bakardjieva, Ch. Motzkus, G. Labarraque, C. Oster, G. Cotogno, C. Gaillard, Multi-walled Carbon Nanotubes, NM-400, NM-401, NM-402, NM-403: Characterisation and Physico-Chemical Properties, Publications Office of the European Union 2014.
 25. T. Oh, J. C. Ku, J.-H. Lee, M. C. Hersam, C. A. Mirkin, *Nano Lett.*, **18**, 6022 (2018).
 26. B. K. Shanbhag, C. Liu, V. S. Haritos, L. He, *ACS Nano*, **12**, 6956 (2018).
 27. Y. W. Chen, C.-H. Lee, Y. L. Wang, T. L. Li, H. C. Chang, *J. Am. Chem. Soc. Langmuir*, **33**, 6521 (2017).
 28. D. J. McClements, *Adv. Colloid Interface Sci.*, **253**, 1 (2018).
 29. C. Andreoli, G. Leter, B. De Berardis, P. Degan, I. De Angelis, F. Pacchierotti, R. Crebelli, F. Barone, A. Zijno, *J. Appl. Toxicol.*, **38**, 1471 (2018).
 30. H. R. Luckarift, M. B. Dickerson, K. H. Sandhage, J. C. Spain, *Small*, **2**, 640 (2006).
 31. N. A. Caveney, F. K. Li, N. C. Strynadka, *Curr. Opin. Struct. Biol.*, **53**, 45 (2018).
 32. C. E. Nanayakkara, J. Pettibone, V. H. Grassian, *Phys. Chem. Chem. Phys.*, **14**, 6957 (2012).
 33. I. Szilágyi, E. Königsberger, P. M. May, *Inorg. Chem.*, **48**, 2200 (2009).
 34. Z. Wang, J. Zeng, G. Tan, J. Liao, L. Zhou, J. Chen, P. Yu, Q. Wang, C. Ning, *Bioact. Mater.*, **3**, 74 (2018).
 35. L. Diaz-Gomez, A. Concheiro, C. Alvarez-Lorenzo, *App. Surf. Sci.*, **452**, 32 (2018).